

Short Communication

Preparation and Corrosion Property of $(\text{Cu}_{50}\text{Zr}_{50})_{(100-x)}\text{Nd}_x$ Amorphous Alloy

Xiang Li¹, Fang Lv¹, Yaoxiang Geng², Fang Qi¹, Yingjie Xu¹, Fang Liu¹, Yuxin Wang^{2,*}

¹ School of Materials Science and Engineering, University of Shanghai for Science and Technology, Shanghai 200093, China

² School of Materials Science and Engineering, Jiangsu University of Science and Technology, Zhenjiang 212003, P. R. China

*E-mail: ywan943@163.com

Received: 25 October 2016 / Accepted: 18 November 2016 / Published: 12 December 2016

Cu-Zr bulk metallic glasses (BMGs) have unique mechanical properties and developed rapidly in recent years. In this paper, a series of $(\text{Cu}_{50}\text{Zr}_{50})_{(100-x)}\text{Nd}_x$ ($0 \leq x \leq 5 \text{at.}\%$) alloys were prepared by using copper mold suction method. Their microstructure and properties were investigated by x-ray diffraction, differential scanning calorimetry, microhardness tester and electrochemical workstation. It was found that $\text{Cu}_{49.5}\text{Zr}_{49.5}\text{Nd}_1$ alloy possesses the best glass forming ability. The addition of Nd element can effectively promote the glass forming ability (GFA) and microhardness of Cu-Zr-Nd alloys. The influence of Nd element on the corrosion resistance of Cu-Zr-Nd alloys was systematically discussed.

Keywords: Cu-Zr bulk metallic glasses, Glass forming ability, Corrosion resistance

1. INTRODUCTION

Bulk metallic glasses have been widely used in many applications due to their unique properties such as: high strength, excellent magnetic property and good corrosion resistance [1-3]. Cu-Zr bulk metallic glasses have good mechanical property and can be fabricated with a relatively low cost. However, further application of Cu-Zr glasses was restricted by their critical size. It is hard to achieve a relatively large size when fabricated under normal process [4-7]. Recently, it was reported that proper addition of rare elements in the glass can significantly increase the glass forming ability and thermal stability. Rare elements have relatively large atomic size and strong binding ability with oxygen atoms. The addition of rare elements can also increase the atomic size difference of glass [8-11].

The atomic ratio of Cu/Zr and Zr/Nd are 0.727 and 0.818, respectively. Meanwhile, according to the related data of mixing heat [3], Cu-Zr-Nd alloy system is well suited for the three empirical principles of amorphous alloy. The addition of Nd should increase the efficiency of atomic deposition and improve the thermal stability of alloy system in the supercooled liquid region. In present research, Nd elements were added into the Cu-Zr alloy system in order to improve their glass forming ability. Cu-Zr-Nd alloys with six different compositions were prepared. Their microstructure, glass forming ability, mechanical property and corrosion resistance were systemically studied.

2. EXPERIMENTAL DETAILS

2.1 Sample preparation

Alloy ingots with compositions of $(\text{Cu}_{50}\text{Zr}_{50})_{(100-x)}\text{Nd}_x$ ($x=0, 1, 2, 3, 4, 5$) were prepared by arc melting under argon atmosphere. The purities of elements used for sample preparation are 99.999 mass%. Each ingot was melted for 5 times in order to achieve a uniform distribution of alloy elements. Alloy rods with a same diameter of 3mm were prepared by copper mold suction casting under a current density range of 90-350A. Alloy rods were mechanically polished up to a mirror finish and then were ultrasonic cleaned for characterization.

2.2 Sample characterization

The phase structure of alloy rods were determined by using a Bruker D8 Focus X-ray diffractometer (XRD, Cu- K_α radiation, $\lambda = 0.15406$ nm). The thermal properties of the glassy alloys, such as the glass transition temperature (T_g), crystallization temperature (T_x) and liquidus temperature (T_l), were measured by Differential Scanning Calorimetry (DSC) technique. The DSC curves were obtained at a heating rate of 20 K/min under Helium atmosphere. The mechanical property of alloy rods was examined by Vickers microhardness tester under a load of 100g with a holding time of 15s. The results for the hardness were the average of 10 measurements. The electrochemical tests were conducted in an electrochemical workstation (PARSTAT 2273) using a classical three-electrode system. Potentiodynamic polarization was measured at room temperature in 0.1mol/L NaCl solution under a scanning rate of 0.33mV/s. The exposed surface area of samples was 1 cm².

3. RESULTS AND DISCUSSION

3.1 Microstructure

Fig. 1 shows the XRD patterns of $(\text{Cu}_{50}\text{Zr}_{50})_{(100-x)}\text{Nd}_x$ ($x=0, 1, 2, 3, 4, 5$) alloys. $\text{Cu}_{50}\text{Zr}_{50}$ alloy has a semi-crystalline structure with a predominant phase of ZrCu. The addition of Nd causes a significant variation of alloy phase structure. $\text{Cu}_{49.5}\text{Zr}_{49.5}\text{Nd}_1$ has a broadening diffraction spectrum

with 2 broaden peaks in the range of 35-40°. Further increasing the amount of Nd led to an obvious crystalline of alloys. The peaks which allocated to ZrCu grow sharper and sharper.

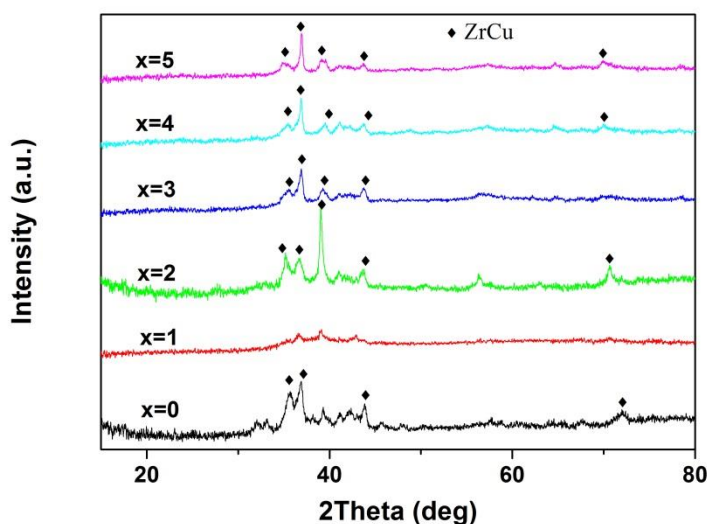


Figure 1. XRD spectrum of $(\text{Cu}_{50}\text{Zr}_{50})_{(100-x)}\text{Nd}_x$ ($x=0, 1, 2, 3, 4, 5$) alloys

3.2 Glass forming ability

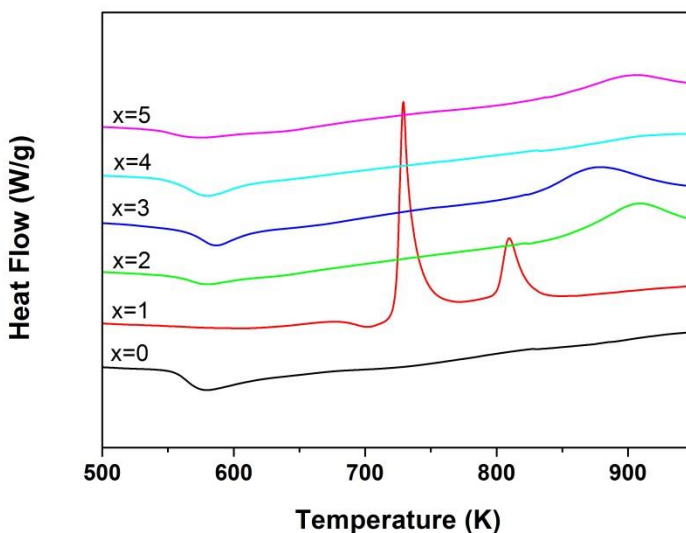


Figure 2. DSC curves of $(\text{Cu}_{50}\text{Zr}_{50})_{(100-x)}\text{Nd}_x$ ($x=0, 1, 2, 3, 4, 5$) alloys with a heating rate of 20 K/min

Fig. 2 presents the DSC curves of $(\text{Cu}_{50}\text{Zr}_{50})_{(100-x)}\text{Nd}_x$ ($x=0, 1, 2, 3, 4, 5$) alloys. No exothermic peak can be seen in $\text{Cu}_{50}\text{Zr}_{50}$ and $\text{Cu}_{48}\text{Zr}_{48}\text{Nd}_4$ alloys, indicating a high degree of crystallization. In contrast, there exists a small exothermic peak in $\text{Cu}_{49}\text{Zr}_{49}\text{Nd}_2$, $\text{Cu}_{48.5}\text{Zr}_{48.5}\text{Nd}_3$ and $\text{Cu}_{47.5}\text{Zr}_{47.5}\text{Nd}_5$ alloys, presenting a semi-crystalline microstructure. $\text{Cu}_{49.5}\text{Zr}_{49.5}\text{Nd}_1$ displayed two exothermic crystallization peaks on the DSC curve, indicating a crystallization process with two steps.

Table 1. Thermal parameters of $\text{Cu}_{49.5}\text{Zr}_{49.5}\text{Nd}_1$ alloy and the other Cu-Zr based BMG alloys

Composition	T_g/K	T_{x1}/K	$\Delta T_x/\text{K}$
$\text{Cu}_{49.5}\text{Zr}_{49.5}\text{Nd}_1$	665	726	61
$\text{Cu}_{48}\text{Zr}_{46}\text{Al}_6$	436	490.3	54.3
$\text{Cu}_{48}\text{Zr}_{45}\text{Al}_7$	437.1	498.1	61
$\text{Cu}_{48}\text{Zr}_{44}\text{Al}_8$	441.6	501.2	59.6
$\text{Cu}_{48}\text{Zr}_{43}\text{Al}_9$	443.5	504.1	60.6
$\text{Cu}_{48}\text{Zr}_{42}\text{Al}_{10}$	440.7	500.2	59.5

Thermal parameters of $\text{Cu}_{49.5}\text{Zr}_{49.5}\text{Nd}_1$ alloy obtained from the DSC curve with the existing results of Cu-Zr based BMG alloys are shown in Table 1 [3, 12-15]. The glass transition temperature (T_g) and the initial crystallization temperature of $\text{Cu}_{49.5}\text{Zr}_{49.5}\text{Nd}_1$ are 665 K and 726 K, respectively. The corresponding supercooled liquid region (ΔT_x) is 61 K, indicating a good thermal stability. It can be seen that the ΔT_x value of $\text{Cu}_{49.5}\text{Zr}_{49.5}\text{Nd}_1$ is higher than the other Cu-Zr based BMG alloys. The addition of Nd can effectively improve the glass forming ability of $\text{Cu}_{50}\text{Zr}_{50}$ alloy.

3.3 Mechanical property

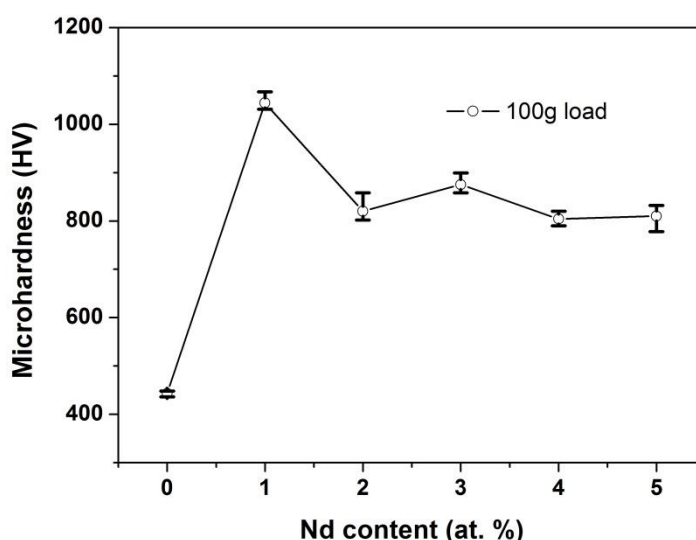
**Figure 3.** Microhardness of $(\text{Cu}_{50}\text{Zr}_{50})_{(100-x)}\text{Nd}_x$ ($x=0, 1, 2, 3, 4, 5$) alloys

Fig. 3 presents the microhardness of $(\text{Cu}_{50}\text{Zr}_{50})_{(100-x)}\text{Nd}_x$ ($x=0, 1, 2, 3, 4, 5$) alloys. $\text{Cu}_{50}\text{Zr}_{50}$ alloy has a relatively low hardness of $\sim 443 \text{ HV}_{100}$. After adding Nd, the microhardness of alloys was significantly improved. The strengthening mechanism can be attributed to the structural evolution of

alloys caused by Nd addition. Proper addition of Nd can promote the formation of glass phase in the alloy. $\text{Cu}_{49.5}\text{Zr}_{49.5}\text{Nd}_1$ alloy possesses the highest microhardness of $\sim 1044 \text{ HV}_{100}$ as it has good glass forming ability. However, further addition of Nd led to a decrease of microhardness but still keep at the level of $\sim 800 \text{ HV}_{100}$. The variation of microhardness is corresponding with the evolution of XRD and DSC results.

3.4 Corrosion property

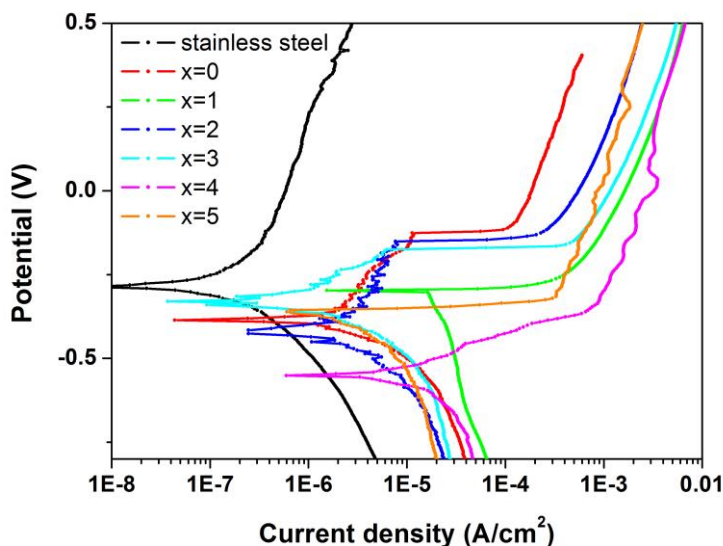


Figure 4. Potentiodynamic polarization curves of $(\text{Cu}_{50}\text{Zr}_{50})_{(100-x)}\text{Nd}_x$ ($x=0, 1, 2, 3, 4, 5$) alloys in 0.1mol/L NaCl solution with a scanning rate of 0.33mV/s

Table 2. Results of potentiodynamic corrosion tests in 0.1mol/L NaCl solution with a scanning rate of 0.33mV/s

Sample	E_{corr} (V vs. SCE)	I_{corr} (A/cm^2)
Stainless steel	-0.28	2.42×10^{-7}
$\text{Cu}_{50}\text{Zr}_{50}$	-0.39	1.66×10^{-6}
$\text{Cu}_{49.5}\text{Zr}_{49.5}\text{Nd}_1$	-0.3	1.74×10^{-5}
$\text{Cu}_{49}\text{Zr}_{49}\text{Nd}_2$	-0.41	1.39×10^{-6}
$\text{Cu}_{48.5}\text{Zr}_{48.5}\text{Nd}_3$	-0.33	3.18×10^{-7}
$\text{Cu}_{48}\text{Zr}_{48}\text{Nd}_4$	-0.55	3.47×10^{-6}
$\text{Cu}_{47.5}\text{Zr}_{47.5}\text{Nd}_5$	-0.36	1.39×10^{-6}

Fig. 4 shows the potentiodynamic polarization curves of $(\text{Cu}_{50}\text{Zr}_{50})_{(100-x)}\text{Nd}_x$ ($x=0, 1, 2, 3, 4, 5$) alloys. The results of potentiodynamic corrosion tests are shown in Table 2. It can be seen that the corrosion potential of $(\text{Cu}_{50}\text{Zr}_{50})_{(100-x)}\text{Nd}_x$ ($x=0, 1, 2, 3, 4, 5$) alloys are lower and their corrosion current density are higher than that of stainless steel. Among $(\text{Cu}_{50}\text{Zr}_{50})_{(100-x)}\text{Nd}_x$ ($x=0, 1, 2, 3, 4, 5$) alloys, $\text{Cu}_{49.5}\text{Zr}_{49.5}\text{Nd}_1$ alloy possesses the highest corrosion potential, while $\text{Cu}_{48.5}\text{Zr}_{48.5}\text{Nd}_3$ has the lowest corrosion current density. No passivation area can be seen in the polarization curve of $\text{Cu}_{49.5}\text{Zr}_{49.5}\text{Nd}_1$ alloy, indicating no passive film was formed on its surface. $\text{Cu}_{50}\text{Zr}_{50}$ and $\text{Cu}_{49}\text{Zr}_{49}\text{Nd}_2$ alloys have a relative broad passivation area in their polarization curve, indicating a passive film was formed on their surface and a relative better corrosion resistance.

There isn't a linear relationship between Nd addition and corrosion resistance of $(\text{Cu}_{50}\text{Zr}_{50})_{(100-x)}\text{Nd}_x$ alloys. Zr is easier to be passivated than Cu and Nd. The passive film of ZrO is dense and stable. $\text{Cu}_{50}\text{Zr}_{50}$ has the best corrosion resistance as it has a low corrosion current density and relative broad passivation area. After adding Nd, the corrosion resistance of $(\text{Cu}_{50}\text{Zr}_{50})_{(100-x)}\text{Nd}_x$ ($x=1, 2, 3, 4, 5$) can't compare with that of $\text{Cu}_{50}\text{Zr}_{50}$ alloy. The reason could be attributed to that Nd is chemically reactive and NdO can't provide good protection for the alloy surface [16-18]. Further investigations are being conducted to study the corrosion mechanism of Cu-Zr-Nd alloy system in order to broaden its application.

4. CONCLUSION

$(\text{Cu}_{50}\text{Zr}_{50})_{(100-x)}\text{Nd}_x$ ($0 \leq x \leq 5 \text{at.}\%$) alloys were prepared by using copper mold suction method. Their microstructure, glass forming ability, mechanical property and corrosion resistance were systematically investigated. The results show that proper addition of Nd element can effectively improve the glass forming ability and mechanical property of Cu-Zr-Nd alloys. $\text{Cu}_{49.5}\text{Zr}_{49.5}\text{Nd}_1$ has the best glass forming ability and highest microhardness. However, the corrosion resistance of Cu-Zr alloys can't be improved by the addition of Nd. Further research on the corrosion mechanism of Cu-Zr-Nd alloys is being conducted to find a broader application in industry.

ACKNOWLEDGEMENT

This work is supported by the financial support from the National Natural Science Foundation of China (No. 51202146 and 51601073).

References

1. A. Inoue and A. Takeuchi, *Acta. Mater.*, 59 (2011) 2243-2267.
2. C. A. Schuh, T. C. Hufnagel and U. Ramamurty, *Acta. Mater.*, 55 (2007) 4067-4109.
3. Y. Q. Cheng and E. Ma, *Prog. Mater. Sci.*, 56 (2011) 379-473.
4. D. Wang, Y. Li, B. B. Sun, M. L. Sui, K. Lu and E. Ma, *Appl. Phys. Lett.*, 84 (2004) 4029-4031.
5. A. L. Zhang, D. Chen and Z. H. Chen, *J. Alloy. Compd.*, 477 (2009) 432-435.
6. M. Wakeda, Y. Shibutani, S. Ogata and J. Park, *Intermetallics.*, 15 (2007) 139-144.
7. O. J. Kwon, Y. C. Kim, K. B. Kim, Y. K. Lee and E. Fleury, *Met. Mater. Int.*, 12 (2006) 207-212.
8. L. Yang and G. Q. Guo, *Appl. Phys. Lett.*, 97 (2010) 091901.

9. Z. Q. Liu, R. Li, G. Liu, W. H. Su, H. Wang, Y. Li, M. J. Shi, X. K. Luo, G. J. Wu and T. Zhang, *Acta. Mater.*, 60 (2012) 3128-3139.
10. S. Gonzalez, *J. Mater. Res.*, 31 (2015) 76-87.
11. P. Yu, H. Y. Bai and W. H. Wang, *J. Mater. Res.*, 21 (2006) 1674-1679.
12. Q. Wang, J. B. Qiang, J. H. Xia, J. Wu, Y. M. Wang and C. Dong, *Intermetallics.*, 15 (2007) 711-715.
13. D. Wang, H. Tan and Y. Li, *Acta. Mater.*, 53 (2005) 2969-2979.
14. A. L. Zhang, D. Chen and Z. H. Chen, *Phil. Mag. Lett.*, 93 (2013) 283-291.
15. I. Kaban, P. Jóvári, B. Escher, D. T. Tran, G. Svensson, M. A. Webb, T. Z. Regier, V. Kokotin, B. Beuneu, T. Gemming and J. Eckert, *Acta. Mater.*, 100 (2015) 369-376.
16. C. Z. Zhang, N. N. Qiu, L. L. Kong, X. D. Yang and H. P. Li, *J. Alloy. Compd.*, 645 (2015) 487-490.
17. H. B. Lu, L. C. Zhang, A. Gebert and L. Schultz, *J. Alloy. Compd.*, 462 (2008) 60-67.
18. Z. T. Zhang, E. Axinte, W. J. Ge, C. Y. Shang and Y. Wang, *Mater. Des.*, 108 (2016) 106-113.

© 2017 The Authors. Published by ESG (www.electrochemsci.org). This article is an open access article distributed under the terms and conditions of the Creative Commons Attribution license (<http://creativecommons.org/licenses/by/4.0/>).